Cardiac H11 kinase/Hsp22 stimulates oxidative phosphorylation and modulates mitochondrial reactive oxygen species production: Involvement of a nitric oxide-dependent mechanism.

Lydie Laure, Romain Long, Paulo Lizano, Roland Zini, Alain Berdeaux, Christophe Depré, Didier Morin

Cardiac H11 kinase/Hsp22 stimulates oxidative phosphorylation and modulates mitochondrial reactive oxygen species production: involvement of a nitric oxide-dependent mechanism.

Lydie Laure[1*], Romain Long[1*], Paulo Lizano[2], Roland Zini[1], Alain Berdeaux[1], Christophe Depre[2], Didier Morin[1]

[1]INSERM, U955, équipe 03 et Université Paris-Est, Faculté de Médecine, F-94010, Créteil-France; [2]Cardiovascular Research Institute, Department of Cell Biology and Molecular Medicine, University of Medicine and Dentistry New Jersey, New Jersey Medical School, Newark, NJ.

*Both authors contributed equally to the work.

To whom correspondence should be addressed:
Didier Morin, PhD, Faculté de Médecine de Créteil, INSERM U955-équipe 03, 8 rue du Général Sarrail, 94010 Créteil Cedex, France. Fax: +33 (0) 1 48 98 17 77. Email: didier.morin@inserm.fr

The abbreviations used are: FCCP, carbonyl cyanide 4-trifluoromethoxyphenylhydrazone; H2O2, hydrogen peroxide; IPC, ischemic preconditioning; L-NAME, L-NG-Nitroarginine Methyl Ester; MRC, mitochondrial respiratory chain; NO, nitric oxide; NOS, nitric oxide synthase; iNOS, inducible isoform of nitric oxide; PTIO, phenyl-tetramethylimidazoline-1-oxyl-3oxide; ROS, reactive oxygen species; TG, transgenic; WT, wild type.

Abstract

H11 Kinase/Hsp22 (Hsp22), a small heat shock protein upregulated by ischemia/reperfusion, provides cardioprotection equal to ischemic preconditioning (IPC) through a nitric oxide (NO)-dependent mechanism. A main target of NO-mediated preconditioning is the mitochondria, where NO reduces O_2 consumption and reactive oxygen species (ROS) production during ischemia. Therefore, we tested the hypothesis that Hsp22 over-expression modulates mitochondrial function through an NO-sensitive mechanism. In cardiac mitochondria isolated from transgenic (TG) mice with cardiac-specific over-expression of Hsp22, mitochondrial basal, ADP-dependent and uncoupled O_2 consumption were increased in the presence of either glucidic or lipidic substrates. This was associated with a decrease in the maximal capabilities of complexes I and III to generate superoxide anion in combination with an inhibition of superoxide anion production by the reverse electron flow. NO synthase (NOS) expression and NO production were increased in mitochondria from TG mice. Hsp22-induced increase in O_2 consumption was abolished by either pretreatment of TG mice with the NO synthase inhibitor L-NG-Nitroarginine Methyl Ester (L-NAME) or in isolated mitochondria by the NO scavenger phenyl-tetramethylimidazoline-1-oxyl-3oxide (PTIO). L-NAME pretreatment also restored the reverse electron flow. After anoxia, mitochondria from TG mice showed a reduction in both oxidative phosphorylation and H_2O_2 production, an effect partially reversed by L-NAME. Taken together, these results demonstrate that Hsp22 over-expression increases the capacity of mitochondria to produce NO, which stimulates oxidative phosphorylation in normoxia and decreases oxidative phosphorylation and ROS production after anoxia. Such characteristics replicate those conferred by IPC, thereby placing Hsp22 as a potential tool for prophylactic protection of mitochondrial function during ischemia.

Keywords: H11 Kinase, heart, heat shock protein, mitochondria, nitric oxide, oxidative phosphorylation, reactive oxygen species

Introduction

Hsp22 is a small molecular weight heat shock protein preferentially expressed in the heart [1,2]. Hsp22 transcript and protein expression is up-regulated in different models of ischemia, both in swine and patients [3,4]. These data support the hypothesis that Hsp22 may promote cell survival in a context of acute, repetitive and chronic ischemia.

A transgenic (TG) mouse with cardiac-specific over-expression of Hsp22 was generated to reproduce the increased expression found in patients [5]. The molecular characteristics of the TG mouse reproduce many hallmarks of IPC, including an activation of cell survival pathways, up-regulation of heat shock proteins, inhibition of pro-apoptotic proteins, metabolic adaptation and stimulation of growth pathways [6-10]. In particular, over-expression of Hsp22 is accompanied by an increased expression of the inducible isoform of nitric oxide (NO) synthase (iNOS) [6], the mediator of the delayed window of IPC [11] and preemptive conditioning of the swine heart by Hsp22 provides cardiac protection through iNOS [12]. A crucial and emerging aspect of the mechanisms of cardioprotection by IPC relies on an NO-mediated adaptation in mitochondrial respiratory function. It was proposed that NO could interact with components of the electron transport chain reducing the generation of reactive oxygen species (ROS) and thereby decreasing the probability for mitochondrial permeability transition pore opening, a major promoter of cell death due to mitochondrial damage [13,14].

Therefore, in the present study we used the TG mouse mentioned above to explore the hypothesis that an NO-dependent adaptation of mitochondrial function, more particularly oxidative phosphorylation and ROS production, could participate in the cardioprotective effect conferred by Hsp22 over-expression.

Material and Methods

Animal model

We used TG female mice (3- to 4-months old), expressing the coding sequence of human Hsp22 and a C-terminal hemagglutinin tag, and their wild type (WT) littermates [7]. When indicated, mice were treated with the NO synthase inhibitor L-NG-nitroarginine methyl ester (L-NAME, 20 mg/kg, i.p.) administered daily for three days before investigation. All animal procedures used in this study were in strict accordance with the European Community Council Directive (86-609/87-848 EEC) and recommendations of the French Ministère de l'Agriculture.

Isolation of fresh cardiac mitochondria

Left ventricular tissue was homogenized in a buffer (220 mM mannitol, 70 mM sucrose, 10 mM HEPES, 2 mM EGTA, pH 7.4 at 4°C) supplemented with 0.25% bovine serum albumin, using a Potter-Elvehjem glass homogenizer in a final volume of 10 ml. The homogenate was filtered through cheese cloth and centrifuged at 1000g for 5 min at 4°C. The supernatant was centrifuged at 10000*g* for 10 min at 4°C. The mitochondrial pellet was resuspended in 50 µl of homogenization buffer without EGTA and bovine serum albumin.

For western blot experiments and determination of mitochondrial NO production, mitochondria were purified on a Percoll® gradient [15] as following. Briefly, the left ventricle cardiac muscle was added to 5 ml of homogenization buffer (sucrose 300 mM, HEPES 10 mM, EGTA 2 mM, pH 7.4 at 4°C) supplemented with 0.25 % bovine serum albumin and including protease, kinase and phosphatase inhibitors. The tissue was sliced and homogenized with a Potter-Elvehjem glass homogenizer by a motor-driven Teflon pestle at 1500 rpm in a final volume of 10 ml. Homogenate was centrifuged at 1100*g* for 5 min at 4°C. The supernatant was centrifuged at 10000*g* for 10 min at 4°C. Mitochondrial pellet was added to 500 µl of homogenization buffer supplemented with 20% Percoll®. Homogenate was centrifuged at 15000*g* for 10 min at 4°C in a final volume of 10 ml. Supernatant was carefully removed and pellet added to 10 ml of homogenization buffer (without Percoll®) before centrifugation at 12000*g* for 5 min at 4°C. The final mitochondrial pellet was added to 50 µl of homogenization buffer in order to obtain a protein concentration of about 20 mg/ml, which was determined using the advanced protein assay reagent kit (FLUKA).

Mitochondrial oxygen consumption

Oxygen consumption of isolated mitochondria was measured at 30°C with a Clark-type electrode fitted to a water-jacketed reaction chamber (Hansatech, Cergy, France). Mitochondria (0.2 mg protein) were incubated in a respiration buffer containing 100 mM KCl, 50 mM sucrose, 10 mM HEPES, 5 mM KH_2PO_4, pH 7.4 at 30°C. The following parameters of mitochondrial respiration were evaluated: 1) Substrate-dependent respiration rate (state 4): oxygen consumption in the presence of either pyruvate/malate (5/5 mM), succinate (5mM) plus rotenone (2µM) or palmitoyl carnitine/malate (5 µM/2 mM); 2) ADP-stimulated respiration rate (state 3): oxygen

consumption in presence of 250 µM ADP); uncoupling respiration in presence of 0.2 µM carbonyl cyanide 4-trifluoromethoxyphenylhydrazone (FCCP).

Measurement of mitochondrial respiratory complexes activity

Mitochondrial respiratory chain enzymatic activities were measured as before [16,17]. Briefly, mitochondrial complex I activity (NADH decylubiquinone oxidoreductase) was measured at 30°C by monitoring the decrease in absorbance resulting from the oxidation of NADH at 340nm. The incubation medium contained 25 mM KH_2PO_4, 5 mM MgCl2, 100 µM decylubiquinone, 250 µM KCN, 1 mg/ml bovine serum albumin and 0.1 mg/ml of freeze-thawed heart mitochondria. The reaction was started by the addition of 200 µM NADH. Mitochondrial complex II activity (succinate ubiquinone reductase) was measured by monitoring the absorbance changes of 2,6-dichloroindophenol at 600 nm. The assay mixture contained 10 mM KH_2PO_4, 2 mM EDTA, 2 µM rotenone, 6 mM succinate, 250 µM KCN, 1 mg/ml bovine serum albumin and 0.033 mg/ml of freeze-thawed heart mitochondria. After a preincubation period of 5 min, the activity of the complex was measured in the presence of 80 µM 2,6-dichloroindophenol. Ubiquinol cytochrome c reductase activity (complex III) was measured as the rate of cytochrome c reduction at 550 nm. The reaction mixture contained 10 mM KH_2PO_4, 2 mM EDTA, 2 µM rotenone, 250 µM KCN, 1 mg/ml bovine serum albumin, 40 µM oxidized cytochrome c, 0.017 mg/ml of freeze-thawed heart mitochondria. The reaction was started by the addition of 100 µM decylubiquinol. Mitochondrial complex IV activity (cytochrome c oxidase) was performed at 550 nm following the decrease in absorbance resulting from the oxidation of reduced cytochrome c.

Determination of mitochondrial reactive oxygen species production

ROS generation was assessed by measuring the rate of hydrogen peroxide (H_2O_2) production. This was determined fluorometrically by the oxidation of amplex red to fluorescent resorufin, coupled to the enzymatic reduction of H_2O_2 by horseradish peroxidase. Essentially, superoxide anion generated in mitochondria was converted endogenously to H_2O_2 and then measured by the assay. Briefly, amplex red (10 µM) and horseradish peroxidase (1 U/ml) were added to isolated mitochondria (0.2 mg protein) in the respiration buffer maintained at 30°C. The reaction was initiated by addition of the respiratory substrates (pyruvate/malate or succinate, 5 mM). The

subsequent increase in fluorescence was monitored over time using a fluorescence spectrometer (Perkin-Elmer SA LS 50B, excitation wavelength 563 nm; emission wavelength 587 nm). Known amounts of H_2O_2 were used to generate standard curves to calculate the rate of H_2O_2 production in nmol/min/mg of mitochondrial protein.

Evaluation of mPTP opening

mPTP opening was studied by analyzing mitochondrial swelling assessed by measuring the change in absorbance at 540 nm (A_{540}) using a Jasco V-530 spectrophotometer. Experiments were carried out at 30°C in 1 ml of respiration buffer with addition of pyruvate/malate (5/5 mM). Mitochondria (0.4 mg/ml) were incubated for 1 min in the respiration buffer and swelling was induced by addition of increasing concentrations of calcium.

Determination of mitochondrial nitric oxide production

NO production of isolated myocardial mitochondria was determined as previously described [18]. Briefly, mitochondria (0.5 mg/ml) were incubated in the respiration buffer including calcium (50 µM), DAF-FM (50 µM), superoxide dismutase (250 U/ml) and catalase (350 U/ml) to prevent interference of superoxide anion and H_2O_2. NO production was monitored at 30°C using a temperature-controlled spectrofluorometer (Jasco FP-6300, excitation wavelength 495 nm; emission wavelength 415 nm). DAF specificity to NO was tested by adding increasing concentration of the NO donor diethylamine NONOate (releasing 1.5 moles of NO by mole of NONOate) which induced a rapid and proportional increase in the probe fluorescence. Known amounts of NONOate were used to generate standard curves to calculate the rate of NO production in nmol/min per mg of mitochondrial protein.

In Vitro anoxia/reoxygenation

Isolated mitochondria (0.2 mg protein) were placed in the water-jacketed reaction chamber containing N_2-satured respiration buffer and were maintained at 30°C for 5 min with a constant steam of N_2 above the solution. Reoxygenation was induced by the addition of the respiration oxygenated buffer and mitochondria were incubated for 1 min before measuring oxidative phosphorylation and ROS production.

Measurement of mitochondrial citrate synthase activity

Citrate synthase activity was determined at 412 nm by measuring the initial rate of reaction of liberated Coenzyme A-SH with 5,5'-ditio-bis-2-nitrobenzoic acid. Mitochondria (0.05 mg/ml) were incubated in 10 mM Tris-HCl buffer (pH 7.5 at 37°C) supplemented with 0.2% Triton X-100 and containing 0.2 mM acetyl-CoA and 0.1 mM 5,5'-dithio-bis-2-nitrobenzoic acid in a final volume of 1 ml. The reaction was carried out at 37°C and initiated by the addition of 0.5 mM oxaloacetate. Measurements were made in a Jasco V-530 spectrophotometer.

Western blot analysis

Proteins were denatured by boiling, resolved on SDS-PAGE 10% polyacrylamide gels, and transferred to polyvinylidiene difluoride membranes. Membranes were blocked with 5% non-fat dry milk in a Tris buffer (Tris 10 mM, NaCl 100 mM, pH 7.5) containing 0.05% Tween-20 for 1h at room temperature. Subsequently, membranes were exposed for 2h to either goat polyclonal anti-human Hsp22 antibody (1:500 Abcam), anti-rat/mouse total OxPhos Complex antibody (1:2500 invitrogen), rabbit polyclonal anti-Voltage Dependent Anion Channel antibody (1:1000 Cell Signaling), rabbit polyclonal anti-iNOS (1:1000 Cell Signaling), rabbit polyclonal anti-nNOS (1:1000 Cell Signaling) or rabbit polyclonal anti-PGC-1 alpha antibody (1:1000 Abcam). After incubation with goat anti-mouse (Santa Cruz Biotechnology), donkey anti-goat (Santa Cruz Biotechnology) or goat anti-rabbit (Santa Cruz Biotechnology) as a secondary antibody at 1:5000, blots were revealed by enhanced chemiluminescent reaction (Amersham ECL) and exposed to X-rays films (Amersham Biosciences). Bands were analyzed by densitometry using Image J software.

Quantitative RT-PCR

Hearts were sampled from TG and WT mice. Total RNA was isolated from mouse heart using RNeasy Fibrous Tissue Mini Kit (QIAGEN, Courtaboeuf, France). cDNA was synthesized from 1 µg of total RNA using the SuperScript first strand synthesis system for the RT-PCR kit (Invitrogen, Cergy Pontoise, France) and random oligonucleotides. Expression of genes encoding NADH ubiquinone oxido-reductase (complex I), succinate dehydrogenase subunit A (complex II), ubiquinol cytochrome c reductase (complex III), cytochrome c oxidase polypeptide

IV subunit 1 (complex IV) and ATP synthase subunit alpha (complex V) was monitored by a real-time qRT-PCR method using an Applied Biosystems 7000 Real-Time PCR System. The ubiquitous 18s RNA was used to normalize the data across samples. Its expression was monitored by SYBRGreen incorporation. The primer pairs used for amplification are given in Table 2. Each experiment was performed in duplicate and repeated at least twice.

Statistical analysis

Results are presented as the mean ± SEM for the number of samples indicated in the legends. Statistical comparison was performed using the Student's t test, with a significance for $P<0.05$. Two-way analysis of variance with post-hoc Bonferroni correction was used for multi-group comparison.

Results

Characteristics of the mice

The functional and morphological characteristics of TG mice have been detailed before [5,6,10]. As expected from these previous studies, cardiac hypertrophy was significant in TG mice, as characterized by the left ventricular weight /tibial length ratio that increased from 3.94±0.07 in WT to 5.66±0.09 mg/mm in TG mice ($P<0.01$; n=10). In addition, Figure 1A shows that Hsp22 is over-expressed in cytosolic and mitochondrial fractions of the myocardium of TG mice as compared to WT.

Activation of the mitochondrial respiratory chain in TG mice

The activity of the mitochondrial respiratory chain (MRC) was evaluated in the presence of either glucidic (pyruvate/malate) or lipidic (palmitoyl carnitine) substrates of complex I. As shown in Table 1, TG mice exhibited a significant ($P<0.05$) increase in both states 4 and 3 values in these conditions. A significant increase in state 3 values was also observed when a substrate of complex II (succinate in the presence of rotenone) was used. Addition of the uncoupling agent FCCP further increased MRC activity in TG mice (Table 1) whatever the substrate used. Since these results showed that Hsp22 over-expression increased the activity of MRC, we evaluated the expression of MRC complexes in TG mice by western-blot analysis and qRT-PCR. Immunoblotting showed that MRC complexes were significantly up-regulated compared to WT

mice by ≈ 133 %, 135 % and 160% and 157 % for complex I, II, III and IV, respectively (Figure 1B). Similar results were obtained with mRNA level determination (Figure 1C).

These effects were not related to a difference in mitochondrial concentration between groups, as citrate synthase activity was identical between WT and TG mice (257±24 vs 243±21 µmol/min/mg proteins, n= 10, respectively). This was confirmed by measurement of the abundance of the peroxisome proliferator-activated receptor gamma coactivator-1alpha (PGC-1α), an important regulator of mitochondrial biogenesis which was similar in WT and TG mice (Figure 1B). In addition, stimulation of MRC activity in TG mice can not be ascribed to an increase in activity of mitochondrial complexes since no difference was found between WT and TG mice when we measured the activity of each MRC complex separately (Figure 1D).

Modulation of reactive oxygen species production by Hsp22 over-expression

We studied next the consequences of the increase in MRC activity in TG mice on ROS production. When pyruvate /malate were used as substrates, H_2O_2 release was low but significantly increased in TG mice as compared to WT (Figure 2). The presence of rotenone, a specific inhibitor of complex I acting at the ubiquinone reducing site [19], increased superoxide production in mitochondria from WT and TG mice. This could be due to the rotenone site itself or to an upstream site of the complex such as the flavin or the iron-sulfur cluster sites which are involved in electron transfer [20]. In addition, rotenone abolished the increase in superoxide production observed between WT and TG mice (Figure 2). This result indicates that the higher production of superoxide in mitochondria from TG mice was caused by the rotenone site itself or was located downstream within the MRC and thus abrogated a potential role of upstream sites. Moreover, rotenone-stimulated H_2O_2 production was reduced in mitochondria from TG mice as compared to WT showing that the ability of complex I to generate superoxide in TG mice was restricted when the forward electron transport was blocked. Therefore we analyzed the production of superoxide caused by complex III, the other site of production within the MRC. We used oxidation of succinate in the presence of rotenone to generate H_2O_2 only from complex III. Under these conditions, the rate of H_2O_2 production was similar in WT and TG mice (Figure 2), which is in agreement with the fact that state 4 respiration rates observed in these mice were similar when MRC was stimulated by succinate in the presence of rotenone (Table 1). This suggests that complex III could not be the site for the over-production of superoxide in

mitochondria from TG mice fed with pyruvate/malate. This hypothesis was reinforced by the investigation of the capacity of complex III from TG mice to produce superoxide. This was performed by measuring superoxide production in the presence of antimycin A, an inhibitor of complex III which induces a high superoxide production from the Q_0 center of complex III [21]. Antimycin A-stimulated H_2O_2 generation was strongly decreased in mitochondria from TG mice as compared to WT (Figure 2) indicating that the capacity of complex III to generate superoxide is limited in TG mice when the production is highly stimulated.

As shown in Figure 2, when succinate was used as a substrate instead of pyruvate/malate, the production rate of mitochondrial superoxide was higher in WT than in TG mice. This high rate was abolished by rotenone showing that superoxide production is due to the complex I and is caused by the reverse electron transfer from complex II to complex I as previously shown [22]. Interestingly, the reverse electron transfer was hugely inhibited in mitochondria from TG mice during succinate oxidation.

Taken together these data indicate that Hsp22 over-expression increases the net production of H_2O_2 from mitochondria in the baseline state following the activation of MRC but abolished superoxide production due to reverse electron flow, and decreased the capacity of complex I and III to generate superoxide when their activity is maximized.

Hsp22 over-expression stimulates mitochondrial NO production

Because over-expression of Hsp22 is accompanied by an increased expression of iNOS [6], we analysed the generation of NO from mitochondria of WT and TG mice. These experiments were performed on mitochondria purified on a Percoll® gradient to avoid membrane contamination. Figure 3A shows that myocardial mitochondria prepared from TG mice produced significantly more NO and at a faster rate than WT mice. This effect was inhibited when TG mice were pretreated with L-NAME. In agreement with these results, immunoblotting of mitochondrial proteins showed an increased expression of NOS in TG mice compared to WT, which was detectable using both iNOS- and nNOS-specific antibodies (Figure 3B).

Hsp22 overexpression limits mPTP opening

Given that mitochondrial NO production was reported to protect against mPTP opening, we examined mPTP opening in cardiac mitochondria isolated from WT and TG mice. Figure 4

shows that calcium-induced mitochondrial swelling was decreased in TG mice and this was observed whatever the calcium concentration used. This indicates that Hsp22 over-expression limits mPTP opening.

Regulation of mitochondrial respiration by Hsp22 is NO-dependent

We investigated next whether the changes in MRC activity found in TG mice are due to this difference in NO production. For that purpose, mice were treated with the NOS inhibitor L-NAME daily for three days before preparation of the mitochondria and measurement of mitochondrial respiration in both states 3 and 4. L-NAME totally abolished the difference in MRC activity observed between mitochondria from TG and WT mice for both states 3 and 4 using pyruvate/malate as substrates (Figure 5A). A similar result was observed when MRC activity of myocardial mitochondria from TG mice was measured in the presence of the NO scavenger 2-phenyl-tetramethylimidazoline-1-oxyl-3oxide (PTIO) (Figure 5C). However, L-NAME did not affect the production of H_2O_2, either when the respiratory electron chain was fed by pyruvate/malate, when the forward electron transport was blocked by rotenone, or when the generation of H_2O_2 was induced by complex III in the presence of antimycin A (Figure 5B). Conversely, L-NAME suppressed the decrease in H_2O_2 production observed in the presence of succinate in mitochondria from TG mice as compared to WT, i.e. it restored the reverse electron transfer at the level of complexe I (Figure 5B). In order to further characterize the role of NO on reverse electron transport, we performed experiments analyzing the effect of the NO donor NONOate in mitochondria issued from WT mice at concentrations which did not affect respiration. As shown in Figure 5D, addition of increasing concentrations of NONOate decreased H_2O_2 production during succinate oxidation. This was not caused by a direct interaction of NO with superoxide, the precursor of H_2O_2, which could have affected H_2O_2 production, since even the highest concentration of NONOate used did not modify H_2O_2 production in presence of pyruvate/malate as substrates (data not shown). This decrease in H_2O_2 production during succinate oxidation was due to inhibition of the reverse electron flow, a similar effect being observed in the presence of rotenone. In addition, we confirmed that this inhibition was due to NO delivery since PTIO abolished the effect of NONOate. These results demonstrate that reverse electron transport can be inhibited by NO and that NO could be responsible for this inhibition in TG mice.

Mitochondrial respiratory chain under anoxic conditions

The results presented above imply a role for NO in the regulation of mitochondrial respiration by Hsp22. Because the role of NO predominates in ischemic conditions, when oxygen pressure is low [14], the measurement of respiration in isolated mitochondria was repeated after a period of anoxia in presence of pyruvate/malate. After anoxia, mitochondria from TG mice showed a reduction in MRC activity which was significantly more important than that found in corresponding WT mice (Figure 6) when respiration was fully stimulated (state 3 or uncoupled respiration). Anoxia induced an increase in H_2O_2 production that was observed either with complex I or complex II substrates but this effect was reduced in TG compared to WT mice (Figure 7). L-NAME partially reversed the effects of anoxia in mitochondria from TG mice, whereas it had no effect in corresponding preparations issued from WT mice (Figure 6). These results show that anoxia strongly reduces mitochondrial respiration through an NO-sensitive mechanism and this leads to an inhibition of post-anoxia H_2O_2 generation.

Discussion

The present study demonstrates that Hsp22 over-expression modulates MRC in both normoxia and anoxia by a NO-dependent mechanism and that this effect could participate to the cardioprotection conferred by Hsp22 in TG mice. Growing evidence suggests that NO-mediated preconditioning is in large part related to a modulation of mitochondrial function. NO has been shown to inhibit cytochrome c oxidase and cytochrome c release, to increase mitochondrial biogenesis, and to limit ROS synthesis [23,24]. Most of these effects are reproduced by nitrite and by a mitochondria-targeted S-nitrosothiol and administration of these drugs reproduces the protection conferred by IPC by modulating mitochondrial respiration [25,26]. Remarkably, the TG mouse with over-expression of Hsp22 shows an increase in iNOS expression that is exactly in the same range as that observed during an episode of IPC [5]. The cytosolic location of iNOS makes it the isoform of choice to synthesize the NO that will target mitochondria but recent immunohistochemical and biochemical studies [27] show that mitochondria also possess their own NOS and are able to generate NO. The present study confirms these data and demonstrates that mitochondrial NOS abundance was significantly increased in TG mice, indicating that both cytosolic and mitochondrial-derived NO can contribute to the effect of Hsp22 over-expression.

This might explain the ability of cardiac mitochondria of TG mice to resist to mPTP opening since mitochondrial NO was reported to protect against mPTP (18). However, as mitochondrial NOS was detected with both iNOS and nNOS antibodies, we cannot conclude on the identity of this NOS. This is a limitation of the study. On the other hand, further investigations are needed to determine the mechanism by which mitochondrial NOS increases in TG mice.

Our data clearly show that Hsp22 over-expression caused an increase in oxidative phosphorylation when mitochondria are fed with NADH substrates in normoxia. This effect is related to the increased expression of NOS as it was blocked by L-NAME pretreatment of TG mice. An apparent paradox is evident with respect to the interaction of NO and its derivatives with MRC. Indeed, NO was shown to inhibit and not to stimulate mitochondrial respiration mainly through interaction with complex IV [28], indicating that the effect observed in TG mice might be unrelated to a direct interaction of NO at the level of the MRC. However, the increase in oxidative phosphorylation was also blocked by the addition of the NO scavenger PTIO confirming that NO produced within the organelle is responsible for this effect. We were unable to reproduce this stimulating effect in mitochondria issued from WT mice by delivering increasing concentrations of NO by means of NONOate (not shown). This supports the idea that other factors than NO could be involved in this mechanism. We recently found that Hsp22 localizes inside the mitochondria where it co-precipitates with STAT3 [29] which has been recently described to stimulate oxidative phosphorylation [30]. A likely hypothesis may be that NO needs such a complex to exert its effect.

The fact that Hsp22 over-expression is associated with an increase in all complexes of the MRC without change in their respective activity could also contribute to the stimulation of oxidative phosphorylation. It has been shown that NO stimulates mitochondrial biogenesis [31,32] through activation of the transcription factor PGC-1α resulting in an increase in MRC complexes [33]. Given that Hsp22 over-expression neither modifies the quantity of cardiac mitochondria nor the expression of the transcription factor PGC-1α, a role of mitochondrial biogenesis is unlikely. It is therefore possible that such enrichment in mitochondrial complexes found in TG mice may be mediated by NO but independently of mitochondrial biogenesis. Hsp22 over-expression may activate nuclear receptors and transcription factors leading to increased expression of mitochondrial respiratory complexes although we have no data to support such hypothesis at the present time.

Our study also shows that Hsp22 over-expression stimulates mitochondrial ROS generation produced by NADH substrates in normoxia but lessens this ROS production from complex I and III when they are blocked, i.e. in the presence of rotenone and antimycin. This suggests that the maximal capacity of both complexes to generate ROS is decreased in TG mice. This property is observed both in normoxia and after anoxia and is maintained when TG mice are treated with L-NAME, excluding a role of NO. This would be consistent with structural modifications of the complexes which would not alter electron transport in native conditions.

In the same way, Hsp22 over-expression largely attenuates the high rate of superoxide production observed with the complex II substrate succinate. This production of superoxide is also inhibited by rotenone and is caused by the reverse electron flow through complex I under conditions of high protonmotive force [22]. Recent data demonstrate that this process can occur under physiological conditions [34,35] and that persistent reverse electron flow may be associated with aging [36,37]. It may also be a significant factor of ischemia-reperfusion injury since it is largely decreased after ischemia [38]. Reverse electron flow is highly dependent on a high membrane potential. As we did not observe any difference in mitochondrial membrane potential between WT and TG mice (not shown), this cannot explain the decrease in reverse electron flow observed in TG mice. Interestingly, reverse electron flow is restored after L-NAME treatment in TG mice suggesting that NO may occupy a site that limits reverse electron flow in complex I of TG mice without affecting overall electron transport of complex I itself in basal conditions. A similar effect was observed with diphenyleneiodonium which also inhibited ROS production [39]. Consistent with such an effect of NO, we demonstrate that direct NO delivery to isolated mitochondria from WT mice inhibits reverse electron flow. This inhibiting effect of NO could contribute to the cardioprotective effect observed in TG mice as NO-mediated transcient inhibition of complex I activity was involved in its cardioprotective effect [25]. The hypothesis for a protective role of NO in mitochondria from TG mice is also supported by their behavioral in anoxic conditions. Indeed, anoxia strongly reduces mitochondrial respiration from TG mice, an effect which is sensitive to L-NAME treatment, and this leads to a strong inhibition of post-anoxia ROS generation. It should be noted that this inhibition of mitochondrial functions in TG mice during anoxia is similar to that described for nitrite, which also exhibits cardioprotective properties [25] and that pharmacological inhibition of mitochondrial respiration during ischemia was shown to improve post-ischemic reperfusion

injury [40,41]. Thus, mitochondria from TG mice appear naturally protected against ischemic stress and react like mitochondria from WT mice subjected to a protective pharmacological treatment.

In conclusion, the present study demonstrates that Hsp22 over-expression 1) increases the capacity of mitochondria to produce NO which stimulates MRC activity in normoxia and 2) decreases the activity of MRC and its capacity to generate ROS after anoxia. Such characteristics replicate to a large extent those conferred by ischemic preconditioning, thereby placing Hsp22 as a potential tool for prophylactic protection of mitochondrial function during ischemia.

Acknowledgements

L. Laure was supported by a post-doctoral grant from INSERM/AREMCAR. R. Long was supported by a doctoral grant from the Ministère de la Recherche et de la Technologie.

References

[1] Kappe, G.; Verschuure, P.; Philipsen, R.; Staalduinen, A.; Van den Bogaart, P.; Boelens, W.; De Jong, W. Characterization of two novel human small heat shock proteins: protein kinase-related HspB8 and testis-specific HspB9. Biochim. Biophys. Acta. 1520: 1-6; 2001.

[2] Smith, C.; Yu, Y.; Kulka, M.; Aurelian, L. A novel human gene similar to the protein kinase (PK) coding domain of the large subunit of Herpes Simplex virus type 2 ribonucleotide reductase (ICP10) codes for a serine-threonine PK and is expressed in melanoma cells. J. Biol. Chem. 275: 25690-25699; 2000.

[3] Depre. C.; Tomlinson, J.E.; Kudej, R.K.; Gaussin, V.; Thompson, E.; Kim, S.J.; Vatner, D.E.; Topper, J.N.; Vatner, S.F. Gene program for cardiac cell survival induced by transient ischemia in conscious pig. Proc. Natl. Acad. Sci. U S A. 98: 9336-9341; 2001.

[4] Depre, C.; Kim, S.J.; John, A.S.; Huang, Y.; Rimoldi, O.E.; Pepper, J.R.; Dreyfus, G.D.; Gaussin, V.; Pennell, D.J.; Vatner, D.E.; Camici, P.G.; Vatner, S.F. Program of cell survival underlying human and experimental hibernating myocardium. Circ. Res. 95: 433-440; 2004.

[5] Depre, C.; Hase, M.; Gaussin, V.; Zajac, A.; Wang, L.; Hittinger, L.; Ghaleh, B.; Yu, X.; Kudej, R.K.; Wagner, T.; Sadoshima, J.; Vatner, S.F. H11 Kinase is a novel mediator of myocardial hypertrophy in vivo. Circ. Res. 91: 1007-1014; 2002.

[6] Depre, C., Wang, L., Sui, X., Qiu, H., Hong, C., Hedhli, N., Ginion, A., Shah, A., Pelat, M., Bertrand, L., Wagner, T., Gaussin, V., Vatner, S.F. H11 Kinase prevents myocardial infarction by pre-emptive preconditioning of the heart. Circ. Res. 98: 280-288; 2006.

[7] Danan, I.J.; Rashed, E.R.; Depre, C. Therapeutic potential of H11 Kinase for the ischemic heart. Cardiovasc. Drug Revs. 25: 14-29; 2007.

[8] Sui, X.; Li, D.; Qiu, H.; Gaussin, V.; Depre, C. Activation of the bone morphogenetic protein receptor by H11Kinase/Hsp22 promotes cardiac cell growth and survival. Circ. Res. 104: 887-895; 2009.

[9] Wang, L.; Zajac, A.; Hedhli, N.; Depre, C. Increased expression of H11 kinase stimulates glycogen synthesis in the heart. Mol. Cell. Biochem. 265: 71-78; 2004.

[10] Hedhli, N.; Wang, L.; Wang, Q.; Rashed, E.; Tian, Y.; Sui, X.; Madura, K.; Depre, C. Proteasome activation during cardiac hypertrophy by the chaperone H11 Kinase/Hsp22. Cardiovasc. Res. 77: 497-505; 2008.

[11] Bolli, R. Cardioprotective function of inducible nitric oxide synthase and role of nitric oxide in myocardial ischemia and preconditioning: an overview of a decade of research. J. Mol. Cell. Cardiol. 33: 1897-1918; 2001.

[12] Chen, L.; Lizano, P.; Zhao, X.; Sui, X.; Dhar, S.K.; Shen, Y.T.; Vatner, D.E.; Vatner, S.F.; Depre, C. Preemptive conditioning of the swine heart by H11 kinase/Hsp22 provides cardiac protection through inducible nitric oxide synthase. Am. J. Physiol. Heart Circ. Physiol. 300: H1303-1310; 2011.

[13] Jones, S.; Bolli, R. The ubiquitous role of nitric oxide in cardioprotection. J. Mol. Cell. Cardiol. 40: 16-23; 2006.

[14] Halestrap, A.; Clarke, S.; Khaliulin, I. The role of mitochondria in protection of the heart by preconditioning. Biochim. Biophys. Acta. 1767: 1007-1031; 2007.

[15] Townsend, P.A.; Davidson, S.M.; Clarke, S.J.; Khaliulin, I.; Carroll, C.J.; Scarabelli, T.M.; Knight, R.A.; Stephanou, A.; Latchman, D.S.; Halestrap, A.P. Urocortin prevents mitochondrial permeability transition in response to reperfusion injury indirectly by reducing oxidative stress. Am. J. Physiol. Heart Circ. Physiol. 293: H928-H938; 2007.

[16] Lo Iacono, L.; Boczkowski, J.; Zini, R.; Salouage, I.; Berdeaux, A.; Motterlini, R.; Morin, D. A carbon monoxide-releasing molecule (CORM-3) uncouples mitochondrial respiration and modulates the production of reactive oxygen species. Free Radic. Biol. Med. 50:1556-1564; 2011.

[17] Zini, R.; Berdeaux, A.; Morin, D. The differential effects of superoxide anion, hydrogen peroxide and hydroxyl radical on cardiac mitochondrial oxidative phosphorylation. Free Radic. Res. 41: 1159-1166; 2007.

[18] Leite, A.C.; Oliveira, H.C.; Utino, F.L.; Garcia, R.; Alberici, L.C.; Fernandes, M.P.; Castilho, R.F.; Vercesi, A.E. Mitochondria generated nitric oxide protects against permeability transition via formation of membrane protein S-nitrosothiols. Biochim. Biophys. Acta 1797: 1210-1216; 2010.

[19] Degli Esposti, M. Inhibitors of NADH-ubiquinone reductase: an overview. Biochim. Biophys. Acta, 1364: 222-235; 1998.

[20] Ohnishi, S.T.; Ohnishi, T.; Muranaka, S.; Fujita, H.; Kimura, H.; Uemura, K.; Yoshida, K.; Utsumi, K. A possible site of superoxide generation in the complex I segment of rat heart mitochondria. J. Bioenerg. Biomembr. 37: 1-15; 2005.

[21] Ksenzenko, M.; Konstantinov, A.A.; Khomutov, G.B.; Tikhonov, A.N.; Ruuge, E.K. Effect of electron transfer inhibitors on superoxide generation in the cytochrome bc1 site of the mitochondrial respiratory chain. FEBS Lett. 155: 19-24; 1983

[22] Brand, M.D. The sites and topology of mitochondrial superoxide production. Exp. Gerontol. 45: 466-472; 2010.

[23] Brown, G. Regulation of mitochondrial respiration by nitric oxide inhibition of cytochrome c oxidase. Biochim. Biophys. Acta. 1504: 46-57; 2001.

[24] Brown, G. Nitric oxide as a competitive inhibitor of oxygen consumption in the mitochondrial respiratory chain. Acta Physiol. Scand. 168: 667-674; 2000.

[25] Shiva, S.; Sack, M.N.; Greer, J.J.; Duranski, M.; Ringwood, L.A.; Burwell, L.; Wang, X.; MacArthur, P.H.; Shoja, A.; Raghavachari, N.; Calvert, J.W.; Brookes, P.S.; Lefer, D.J.; Gladwin, M.T. Nitrite augments tolerance to ischemia/reperfusion injury via the modulation of mitochondrial electron transfer. J. Exp. Med. 204: 2089-2102; 2007.

[26] Prime, T.A.; Blaikie, F.H.; Evans, C.; Nadtochiy, S.M.; James A.M.; Dahm, C.C.; Vitturi, D.A.; Patel, R.P.; Hiley, C.R.; Abakumova, I.; Requejo, R.; Chouchani, E.T.; Hurd, T.R.; Garvey, J.F.; Taylor, C.T.; Brookes, P.S.; Smith, R.A.; Murphy, M.P. A mitochondria-targeted S-nitrosothiol modulates respiration, nitrosates thiols, and protects against ischemia-reperfusion injury. Proc. Natl. Acad. Sci. U S A. 106:10764-10769; 2009.

[27] Navarro, A.; Boveris, A. Mitochondrial nitric oxide synthase, mitochondrial brain dysfunction in aging, and mitochondria-targeted antioxidants. Adv. Drug Deliv. Rev. 60: 1534-1544; 2008.

[28] Brown, G.C.; Borutaite, V. Nitric oxide and mitochondrial respiration in the heart. Cardiovasc. Res. 75: 283-290; 2007.

[29] Qiu, H.; Lizano, P.; Laure, L.; Sui, X.; Rashed, E.; Park, J.Y.; Hong, C.; Gao, S.; Holle, E.; Morin, D.; Dhar, S.K.; Wagner, T.; Berdeaux, A.; Tian, B.; Vatner, S.F.; Depre, C. H11 Kinase/Heat Shock Protein 22 deletion impairs both nuclear and mitochondrial functions of Stat3 and accelerates the transition into heart failure on cardiac overload. Circulation 124: 406-415; 2011.

[30] Wegrzyn, J.; Potla, R.; Chwae, Y.J.; Sepuri, N.B.; Zhang, Q.; Koeck, T.; Derecka, M.; Szczepanek, K.; Szelag, M.; Gornicka, A.; Moh, A.; Moghaddas, S.; Chen, Q.; Bobbili, S.; Cichy, J.; Dulak, J.; Baker, D.P.; Wolfman, A.; Stuehr, D.; Hassan, M.O.; Fu, X.Y.;

Avadhani, N.; Drake, J.I.; Fawcett, P.; Lesnefsky, E.J.; Larner, A.C. Function of mitochondrial Stat3 in cellular respiration Science 323: 793-797; 2009.

[31] Nisoli, E.; Clementi, E.; Paolucci, C.; Cozzi, V.; Tonello, C.; Sciorati, C.; Bracale, R.; Valerio, A.; Francolini, M.; Moncada, S.; Carruba, M.O. Mitochondrial biogenesis in mammals: the role of endogenous nitric oxide. Science 299: 896-899; 2003.

[32] Nisoli, E.; Falcone, S.; Tonello, C.; Cozzi, V.; Palomba, L.; Fiorani, M.; Pisconti, A.; Brunelli, S.; Cardile, A.; Francolini, M.; Cantoni, O.; Carruba, M.O.; Moncada, S.; Clementi, E. Mitochondrial biogenesis by NO yields functionally active mitochondria in mammals. Proc. Natl. Acad. Sci. U S A. 101; 16507-16512. 2004.

[33] McLeod, C.J.; Pagel, I.; Sack, M.N. The mitochondrial biogenesis regulatory program in cardiac adaptation to ischemia--a putative target for therapeutic intervention. Trends Cardiovasc. Med. 15: 118-123; 2005.

[34] Zoccarato, F.; Cavallini, L.; Bortolami, S.; Alexandre, A. Succinate modulation of H2O2 release at NADH:ubiquinone oxidoreductase (Complex I) in brain mitochondria Biochem. J. 406: 125-129; 2007.

[35] Muller, F.L.; Liu, Y.; Abdul-Ghani, M.A.; Lustgarten, M.S.; Bhattacharya, A.; Jang, Y.C.; Van Remmen, H. High rates of superoxide production in skeletal-muscle mitochondria respiring on both complex I- and complex II-linked substrates.Biochem. J. 409: 491-499; 2008.

[36] Lambert, A.J.; Boysen, H.M.; Buckingham, J.A.; Yang, T.; Podlutsky, A.; Austad, S.N.; Kunz, T.H.; Buffenstein, R.; Brand, M.D. Low rates of hydrogen peroxide production by isolated heart mitochondria associate with long maximum lifespan in vertebrate homeotherms. Aging Cell. 6: 607-618; 2007.

[37] Skulachev, V.P. A biochemical approach to the problem of aging: "megaproject" on membrane-penetrating ions. The first results and prospects. Biochemistry (Mosc) 72: 1385-1396; 2007.

[38] Chen, Q.; Moghaddas, S.; Hoppel, C.L.; Lesnefsky, E.J. Ischemic defects in the electron transport chain increase the production of reactive oxygen species from isolated rat heart mitochondria. Am. J. Physiol. Cell. Physiol. 294: C460-C466; 2008.

[39] Lambert, A.J.; Buckingham, J.A.; Boysen, H.M.; Brand, M.D. Diphenyleneiodonium acutely inhibits reactive oxygen species production by mitochondrial complex I during reverse, but not forward electron transport. Biochim. Biophys. Acta. 1777: 397-403; 2008.

[40] Lesnefsky, E.J.; Chen, Q.; Moghaddas, S.; Hassan, M.O.; Tandler, B.; Hoppel, C.L. Blockade of electron transport during ischemia protects cardiac mitochondria. J. Biol. Chem. 279: 47961-47967; 2004.

[41] Aldakkak, M.; Stowe, D.F.; Chen, Q.; Lesnefsky, E.J.; Camara, A.K. Inhibited mitochondrial respiration by amobarbital during cardiac ischaemia improves redox state and reduces matrix Ca2+ overload and ROS release. Cardiovasc. Res. 77: 406-415; 2008.

Legends for figures

Figure 1. Protein expression and activities of mitochondrial respiratory chain complexes in TG mice. A: Immunoblotting of Hsp22 in cytosolic and mitochondrial myocardial fractions in WT and TG mice. B: Immunoblotting of complexes I, II, III, IV and V and of PGC-1α in mitochondrial fractions from TG and WT mice. Voltage Dependent Anion Channel (VDAC) was used as a loading control. Each value is expressed in percentage of WT value and represents the mean ± S.E.M. of 6 independent preparations. * $P<0.05$ vs WT. C: RNA expression of mitochondrial respiratory chain complexes in TG and WT mice. 18S was used to normalize the data across samples. Each value is expressed in percentage of WT value and represents the mean ± S.E.M. of 4 independent preparations. * $P<0.05$ vs WT. D: enzymatic activity of each respiratory chain complex (µmol/min/mg proteins) measured in mitochondrial fractions prepared from hearts of WT and TG mice. Each value represents the mean ± S.E.M. of 6 independent preparations.

Figure 2. Modulation of reactive oxygen species production in TG mice. H_2O_2 production was induced by pyruvate/malate (P/M, 5/5mM) or succinate (Suc, 5 mM) in the absence or in the presence of either rotenone (Rot, 2 µM) or antimycin (Ant, 2µM) and was determined fluorometrically by the oxidation of amplex red to fluorescent resorufin. Each value represents the mean ± S.E.M. of at least 8 independent preparations; * $P<0.05$ vs WT; ** $P<0.005$ vs WT.

Figure 3. Stimulation of NO production in TG mice. A: NO production by mitochondria was determined fluorometrically using DAF-FM (10 µM) in the presence of SOD (250 U/ml) and catalase (350 U/ml). Curves are representative of 4 experiments. NO production was calculated by measuring the slope of the initial production of each curve. Each value represents the mean ± S.E.M. of at least 4 independent preparations; * $P<0.05$ vs WT; # $P<0.05$ vs TG control mice. B: expression of NOS in mitochondrial fractions from TG and WT mice. Voltage Dependent Anion Channel (VDAC) was used as a loading control. Each value is expressed in percentage of WT value and represents the mean ± S.E.M. of 6 independent preparations. * $P<0.05$ vs WT.

Figure 4. Mitochondrial swelling in TG mice. A: mitochondria isolated from left ventricules of WT and TG mice were incubated in the respiration buffer and swelling was induced by the addition of 500µM calcium (c,d). No addition of calcium (a,b). B: evaluation of mitochondrial swelling in the presence of increasing concentrations of calcium.

Figure 5. NO-dependent regulation of the mitochondrial respiratory chain and of the mitochondrial production of reactive oxygen species in TG mice. A and B: Fresh mitochondria were isolated from left ventricles of WT and TG mice pretreated or not with L-NAME (20mg/kg/day for 3 days). A: O_2 consumption (nmol O_2/min/mg proteins) was induced by pyruvate/malate (P/M, 5/5 mM) in the presence (state 3) or in the absence (state 4) of 0.25 mM ADP. Each value represents the mean ± S.E.M. of 6 independent preparations. * $P<0.05$ vs WT, # $P<0.05$ vs untreated (control, CTL) mice. B: H_2O_2 production was induced by P/M (5/5mM) or succinate (Suc, 5 mM) in the presence of 2 µM rotenone (Rot) and/or 2 µM antimycin (Ant) and was determined fluorometrically. Each value represents the mean ± S.E.M. of at least 8 independent preparations. * $P<0.05$ vs WT; # $P<0.05$ vs respective control (CTL) mice.

C: Fresh mitochondria were isolated from left ventricles of WT and TG mice and O_2 consumption (nmol O_2/min/mg proteins) was induced by P/M (5/5 mM, state 4) or by P/M (5/5mM) + ADP (0.25 mM, state 3) in the absence or in the presence of PTIO (50 µM). Each value represents the mean ± S.E.M. of 5-6 independent preparations. * $P<0.05$ vs WT, # $P<0.05$ vs respective control (CTL) mitochondria.

D: Fresh mitochondria were isolated from left ventricles of WT mice and H_2O_2 production was induced by succinate (5 mM) in the absence (CTL) or in the presence of increasing concentrations of NONOate in mitochondria issued from WT mice. PTIO (50 µM) abolished the effect of NONOate whatever the concentration used. Results are representative of 4 independent experiments.

Figure 6. Mitochondrial respiratory chain after anoxia in TG mice. Fresh mitochondria were isolated from left ventricles of WT and TG mice pretreated or not with L-NAME (20mg/kg/day for 3 days). O_2 consumption was measured in the presence of pyruvate/malate (5/5 mM), in the absence (substrate-dependent state 4) or in the presence of ADP (ADP-stimulated state 3) or

FCCP (uncoupled state). Experiments were performed in normoxic conditions or after 5 min anoxia. Each value represents the mean ± S.E.M. of 6 independent preparations. * P<0.05 vs respective normoxia; # P<0.05 vs respective anoxia.

Figure 7: Reactive oxygen species production after anoxia in TG mice. H_2O_2 production was induced by pyruvate/malate (P/M) or succinate + rotenone (Suc+Rot) and was determined fluorometrically by oxidation of amplex red to fluorescent resorufin. Each value represents the mean ± S.E.M. of 5 independent preparations. * P<0.05 vs respective normoxia; # P<0.05 vs respective anoxia.

Figure 1

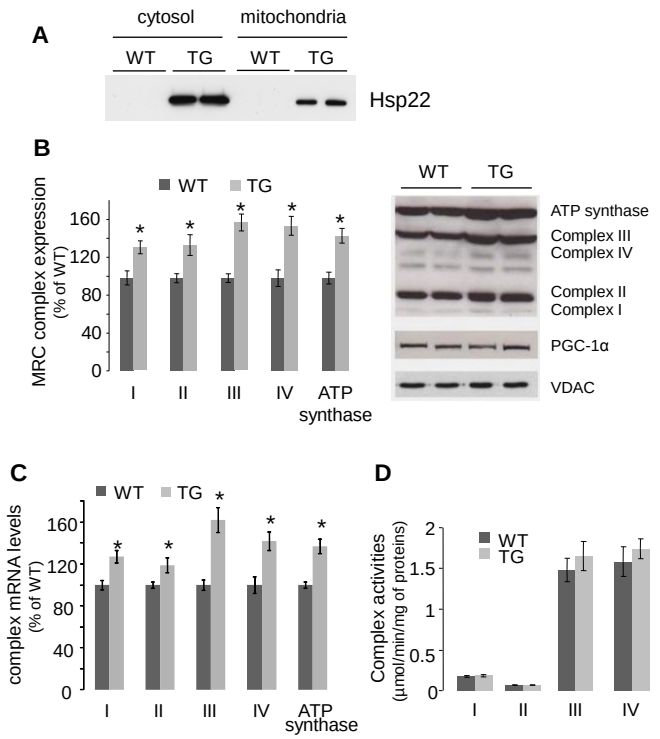
A
cytosol
mitochondria
WT
TG
WT
TG
Hsp22
B
WT
TG
MRC complex expression (% of WT)
160
120
80
40
0
I
II
III
IV
ATP synthase
WT
TG
ATP synthase
Complex III
Complex IV
Complex II
Complex I
PGC-1α
VDAC
C
WT
TG
complex mRNA levels (% of WT)
160
120
80
40
0
I
II
III
IV
ATP synthase
D
Complex activities (μmol/min/mg of proteins)
WT
TG
2
1.5
1
0.5
0
I
II
III
IV

Figure 2

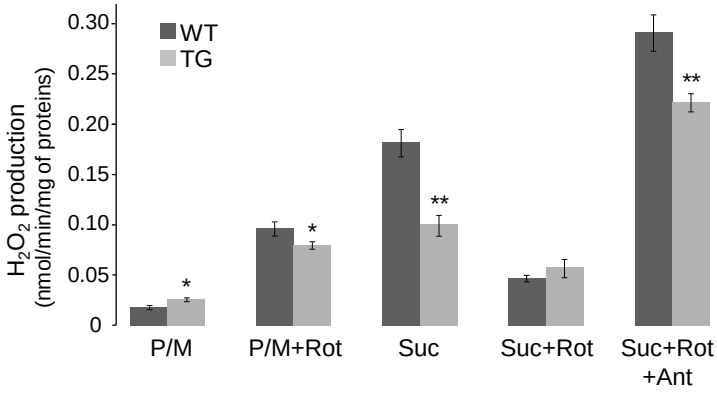
0.30
0.25
0.20
0.15
0.10
0.05
0
WT
TG
H_2O_2 production
(nmol/min/mg of proteins)
*
*
**
**
P/M
P/M+Rot
Suc
Suc+Rot
Suc+Rot
+Ant

Figure 3

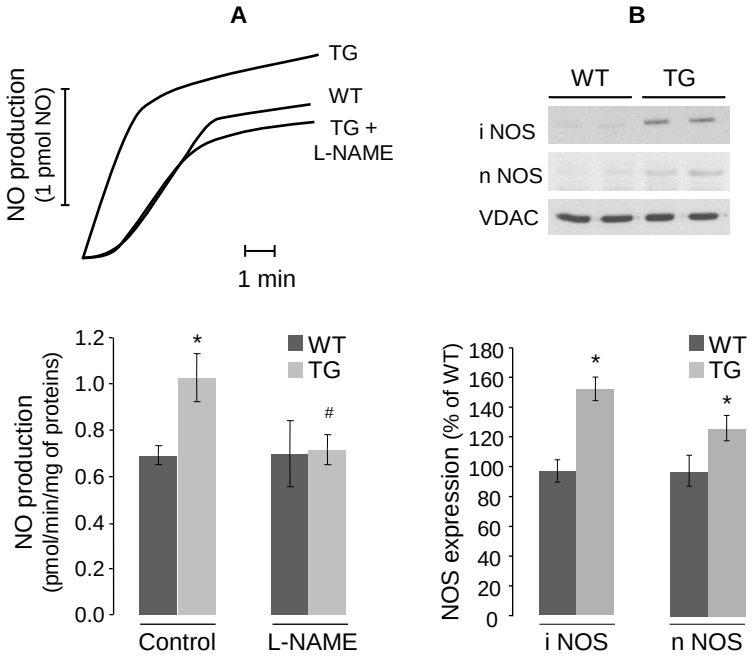
A
B
TG
WT
TG +
L-NAME
NO production
(1 pmol NO)
1 min
WT
TG
i NOS
n NOS
VDAC
NO production
(pmol/min/mg of proteins)
1.2
1.0
0.8
0.6
0.4
0.2
0.0
*
#
WT
TG
Control
L-NAME
NOS expression (% of WT)
180
160
140
120
100
80
60
40
20
0
*
*
WT
TG
i NOS
n NOS

Figure 4

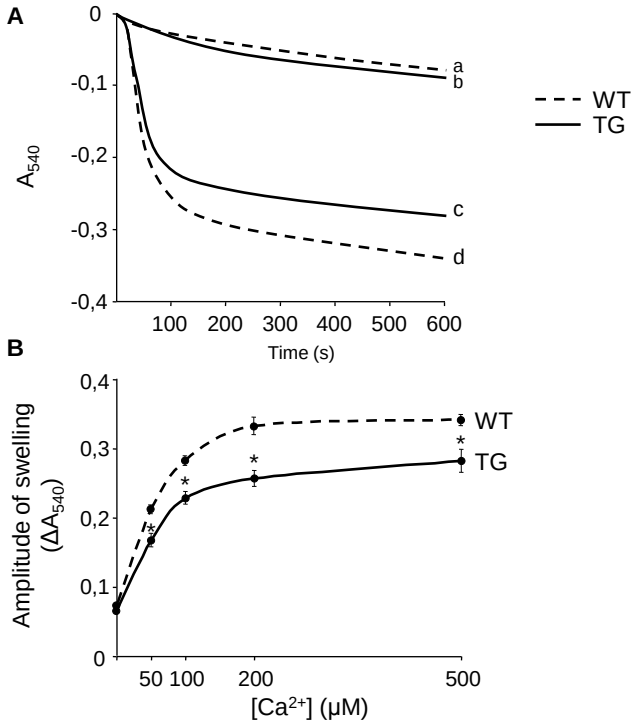
A
0
-0,1
-0,2
-0,3
-0,4
A_{540}
a
b
c
d
100 200 300 400 500 600
Time (s)
WT
TG
B
0,4
0,3
0,2
0,1
0
Amplitude of swelling
(ΔA_{540})
50 100 200 500
$[Ca^{2+}]$ (µM)
WT
TG
*

Figure 5

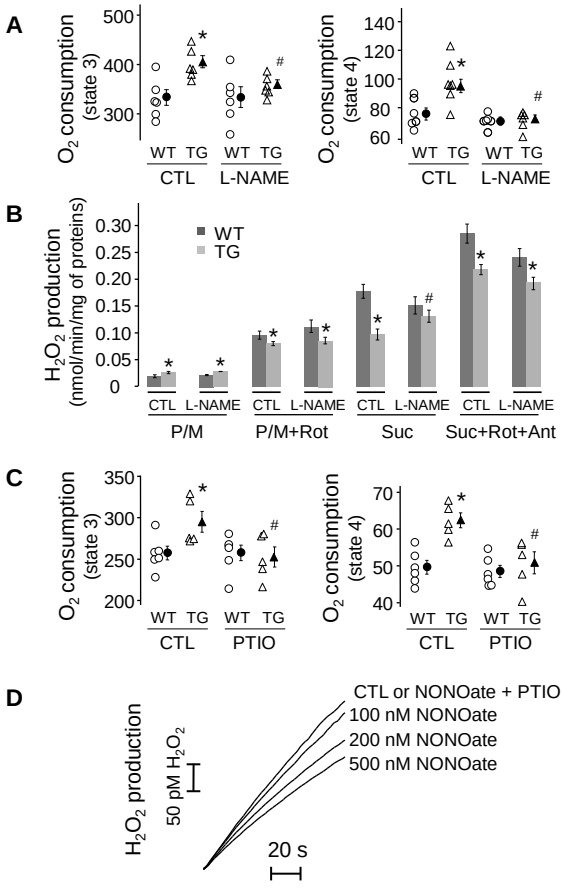
A
O2 consumption (state 3)
500
400
300
WT TG WT TG
CTL L-NAME
O2 consumption (state 4)
140
120
100
80
60
WT TG WT TG
CTL L-NAME
B
H2O2 production (nmol/min/mg of proteins)
0.30
0.25
0.20
0.15
0.10
0.05
0
WT
TG
CTL L-NAME CTL L-NAME CTL L-NAME CTL L-NAME
P/M P/M+Rot Suc Suc+Rot+Ant
C
O2 consumption (state 3)
350
300
250
200
WT TG WT TG
CTL PTIO
O2 consumption (state 4)
70
60
50
40
WT TG WT TG
CTL PTIO
D
H2O2 production
50 pM H2O2
20 s
CTL or NONOate + PTIO
100 nM NONOate
200 nM NONOate
500 nM NONOate

Figure 6

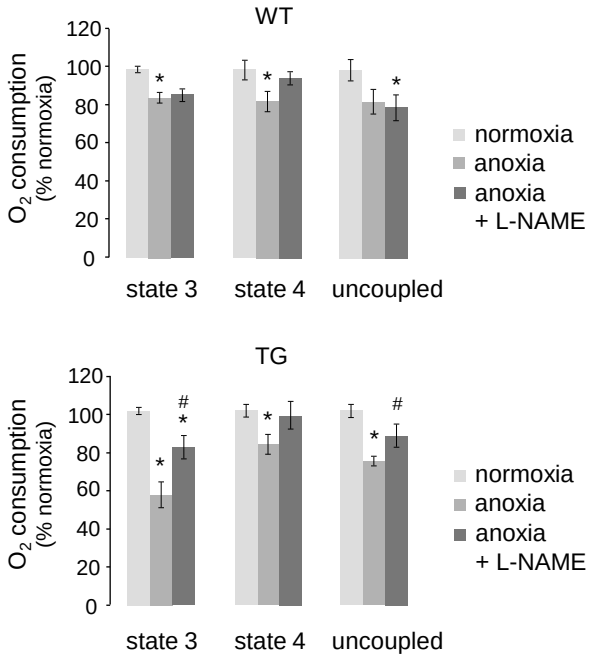
WT
O_2 consumption (% normoxia)
120
100
80
60
40
20
0
*
*
*
state 3
state 4
uncoupled
normoxia
anoxia
anoxia + L-NAME
TG
O_2 consumption (% normoxia)
120
100
80
60
40
20
0
#
*
*
*
#
state 3
state 4
uncoupled
normoxia
anoxia
anoxia + L-NAME

Figure 7

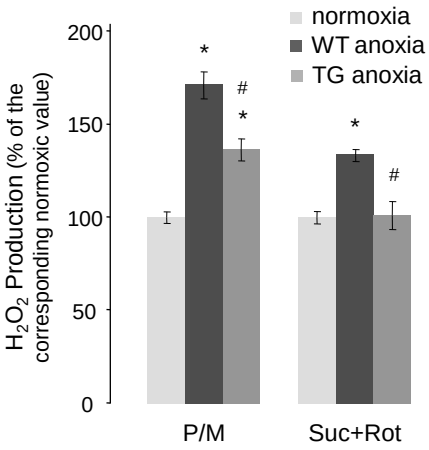
normoxia
WT anoxia
TG anoxia
H_2O_2 Production (% of the corresponding normoxic value)
200
150
100
50
0
*
#
*
*
#
P/M
Suc+Rot

Table 1.

Characterization of mitochondrial respiratory chain activity in TG mice. Substrate-dependent (state 4), ADP-stimulated (state 3) and uncoupled (with FCCP) O_2 consumptions were measured in the presence of glucidic (pyruvate/malate, P/M or succinate + rotenone, Suc+Rot) or lipidic (palmitoyl carnitine, PC) substrates as described under Materials and Methodes. Each value is the mean ± S.E.M. of at least 6 independent mitochondrial preparations; * P<0.05 vs respective WT.

		O_2 consumption (nmol/min/mg proteins)		
		P/M	Suc+Rot	PC
WT	state 4	76 ± 5	142 ± 10	84 ± 8
	state 3	319 ± 11	347 ± 21	336 ± 27
	uncoupled	322 ± 15	-	354 ± 11
TG	state 4	102 ± 5*	149 ± 9	109 ± 8*
	state 3	392 ± 18*	407 ± 5*	467 ± 46*
	uncoupled	408 ± 12*	-	483 ± 51*

Table 2

Primers used for qRT-PCR.

Gene	Primer name	Sequence (5'-> 3')
NADH ubiquinone oxido-reductase	NDUFS7 F	CCCTGTGGCCTATGACCTT
	NDUFS7 R	AGCGTGCCAGCTACAATCAT
succinate dehydrogenase subunit A	SDHA F	CTTGAATGAGGCTGACTGTG
	SDHA R	ATCACATAAGCTGGTCCTGT
ubiquinol cytochrome c reductase	UQCRC2 F	TTCCCTGCTCACTGGCTACT
	UQCRC2 R	TCATGCTCTGGTTCTGATGC
cytochrome c oxidase polypep IV subunit1	COXIV-I F	ACTACCCCTTGCCTGATGTG
	COXIV-I R	GCCCACAACTGTCTTCCATT
ATP synthase subunit alpha	ATP5A1 F	CCTTCCACAAGGAACTCCAA
	ATP5A1 R	GGTAGCTGTTGGTGGGCTAA
18S	18S F	TCCCAGTAAGTGCGGGTCATA
	18S R	CGAGGGCCTCACTAAACCATC